ACS Catalysis

Research Article

pubs.acs.org/acscatalysis

CO_2 Reduction on Supported Ru/Al_2O_3 Catalysts: Cluster Size Dependence of Product Selectivity

Ja Hun Kwak,*[,†,#] Libor Kovarik,[‡] and János Szanyi*[,†]

[†]Institute for Integrated Catalysis, [‡]Environmental Molecular Sciences Laboratory, Pacific Northwest National Laboratory, Richland, Washington 99352, United States

ABSTRACT: The catalytic performance of a series of Ru/Al_2O_3 catalysts with Ru content in the 0.1−5% range was examined in the reduction of CO_2 with H_2. At low Ru loadings (≤0.5%) where the active metal phase is highly dispersed (mostly atomically) on the alumina support, CO is formed with high selectivity. With increasing metal loading, the selectivity toward CH_4 formation increases, while that for CO production decreases. In the 0.1% Ru/Al_2O_3 catalyst, Ru is mostly present in atomic dispersion, as scanning transmission electron microscopy (STEM) images obtained from the fresh sample prior to catalytic testing reveal. STEM images recorded from this same sample, following the temperature programmed reaction test, clearly show the agglomeration of small metal particles (and atoms) into 3D clusters. The clustering of the highly dispersed metal phase is responsible for the observed dramatic selectivity change during elevated temperature tests: dramatic decrease in CO and large increase in CH_4 selectivity. Apparent activation energies, estimated from the slopes of Arrhenius plots, of 82 and 62 kJ/mol for CO and CH_4 formation were determined, respectively, regardless of Ru loading. These results suggest that the formation of CO and CH_4 follow different reaction pathways or proceed on active centers of a different nature. Reactions with CO_2/H_2 and CO/H_2 mixtures (under otherwise identical reaction conditions) reveal that the onset temperature of CO_2 reduction is about 150 °C lower than of CO reduction.

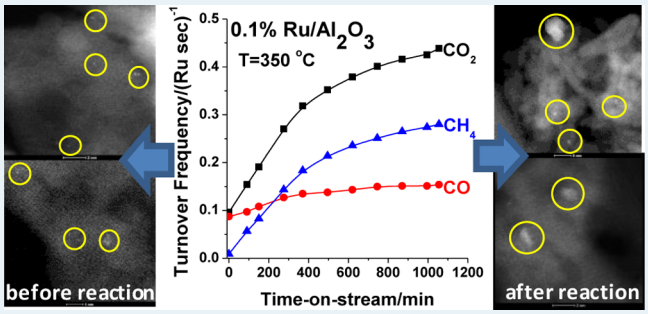

KEYWORDS: *CO_2 reduction, Ru/Al_2O_3, CO/CH_4 selectivity, Ru dispersion, reaction mechanism*

INTRODUCTION

The conversion of CO_2 to high energy density organic molecules (e.g., methanol or methane) has been proposed over both homogeneous and heterogeneous catalysts containing transitions metals (e.g., Cu, Ni, and Pd) as active centers.[1−3] Considerable work has been aimed at designing and synthesizing heterogeneous CO_2 reduction catalysts.[4−8] The activity and selectivity of these catalysts have been shown to be very sensitive to the cluster size and the shape of the metal particles dispersed on the support, as well as to the interaction between the active metals and oxide supports.[9,10] However, these features of oxide-supported metal catalysts remain, to a great extent, hard to control due to the nature of synthetic protocols and, in particular, to sintering of metal clusters during the activation process. The heterogeneous catalytic conversion of CO_2 is currently not feasible due to the demanding reaction conditions (e.g., high catalyst bed temperature) originating from the chemical inertness of CO_2. Therefore, understanding the elementary reaction steps of catalytic CO_2 reduction is critical in order to design economically viable catalytic systems.

Despite the ongoing research efforts, the role of support and the control of CO/CH_4 selectivity in the reduction of CO_2 with H_2 have not been well established, in particular not on subnanometer-sized supported metal atoms/clusters. Recently, we have reported on the very unique catalytic properties of isolated Pd atoms in the reduction of CO_2.[11] In that report, we showed that atomically dispersed supported metals can be catalytically active even in the demanding reaction of CO_2 reduction, but their activity and selectivity patterns differ by a large extent from those of 3D metal particles. The results of CO_2 hydrogenation reaction on Pd/Al_2O_3 and Pd/MWCNT catalysts have unambiguously proved the need of two different functionalities in an active catalyst. The reduction of CO_2 requires the presence of a catalyst component that is able to activate CO_2 (either the support oxide (Al_2O_3) or an oxide promoter) and a metallic component (here Pd) that is able to dissociate H_2. When both of these functionalities are present, the CO and CH_4 selectivities seem to be determined by the sizes of the metal particles.

In this study, we prepared a series of Ru on alumina catalysts with Ru loadings that assured a dispersion range from atomic to 3D clusters and tested their CO_2 reduction performances. Atomically dispersed Ru on alumina initially produced CO exclusively by CO_2 reduction. This is in complete contrast with the catalytic behavior of 3D Ru clusters supported on alumina

Received: May 23, 2013
Revised: September 12, 2013
Published: September 16, 2013

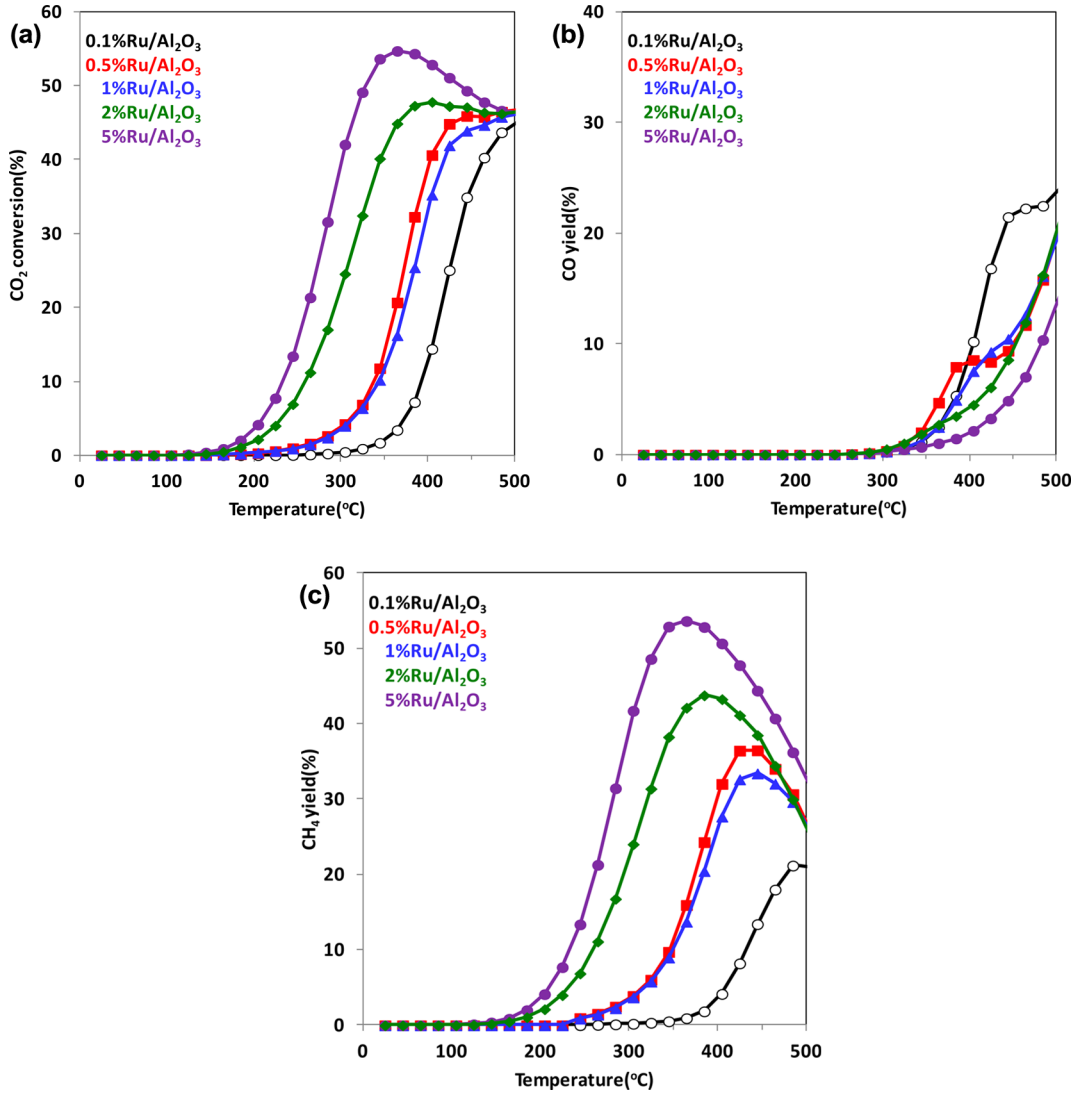

Figure 1. Temperature programmed CO_2 reduction reaction on Ru/Al_2O_3 catalysts: CO_2 conversion (a) and CO (b) and CH_4(c) yields. ($m_{catalyst}$ = 50 mg, 5% CO_2 + 15% H_2 in He (total flow rate = 60 mL/min), heating rate = 5 °C/min.)

that have been known to be efficient methanation catalysts.[12−14] On the basis of these results, we propose that CO can be produced by different reaction mechanisms on active Ru centers with different particle sizes. Furthermore, CO may not be a simple reaction intermediate in the path of CO_2 hydrogenation to CH_4.

EXPERIMENTAL SECTION

Al_2O_3-supported, 00.1, 0.5, 1, 2 and 5 wt % Ru catalysts were prepared on a commercial γ-Al_2O_3 powder (Condea, BET surface area = 200 m^2/g) by the incipient wetness method using ruthenium(III) nitrosyl nitrate solution ($Ru(NO)(NO_3)_x(OH)_y$, $x + y = 3$ in dilute nitric acid, 1.5% Ru, Aldrich) as the precursor. CO_2 reduction activity measurements were conducted by temperature programmed reaction methods in a packed bed reactor using 50 mg of catalyst powder samples (quartz reactor O.D. = 1/2 in.). The catalysts were activated prior to catalytic measurements by calcination at 500 °C for 2 h under 6.7% O_2/He (flow rate = 60 mL/min) and followed by reduction at 500 °C for 30 min under 15% H_2/He (flow rate = 60 mL/min). The activity was measured using a feed gas mixture containing 5% CO_2 and 15% H_2 in He (total flow rate = 60 mL/min and H_2/CO_2 = 3; $m_{catalyst}$= 50 mg). The concentrations of all reactant and product species were measured by a gas chromatograph (HP 7820), with separation using a capillary column (Supelco, Carboxene-1006 PLOT, 30 m × 0.53 mm I.D.) and a thermal conductivity detector. A temperature programmed CO hydrogenation reaction was also performed using 5% CO, with the same protocols.

Catalytic activity changes by sintering were tested by time-on-stream measurements at 350 °C up to 16 h on the 0.1% Ru/Al_2O_3 catalyst prepared by the same pretreatments under the same reaction conditions as described previously. Steady state activities were measured at 280−320 °C, which show stable activities up to 1 h, with different Ru loaded catalysts using newly activated samples for each temperature, and initial activities were extrapolated. Catalytic activities were evaluated under conditions where CO_2 conversion stayed below 5%. Turnover frequencies (TOF, number of CO_2 converted/$Ru_{surface}$·s) were calculated on the basis of the number of surface Ru atoms (as determined from H_2 chemisorption measurements) on alumina. For the H_2 chemisorption experiments, the catalysts were pretreated under identical conditions that were applied prior to the catalytic tests. The

dx.doi.org/10.1021/cs400381f | ACS Catal. 2013, 3, 2449−2455

amount of chemisorbed H_2 was determined on the thus treated samples using a Micromeritics AutoChem 2920 Chemisorption Analyzer apparatus. The activated catalyst (calcined then reduced) was held a 100 °C during H_2 chemisorption measurements.

High-resolution TEM imaging was performed with a FEI Titan 80-300 microscope operated at 300 kV. The instrument is equipped with a CEOS GmbH double-hexapole aberration corrector for the probe-forming lens, which allows imaging with 0.1 nm resolution in scanning transmission electron microscopy (STEM) mode. The images were acquired in high angle annular dark field (HAADF) with an inner collection angle of 52 mrad. The sample preparation for the TEM measurements involved mounting of the powder samples on lacey carbon TEM grids and immediate loading into the TEM airlock to minimize extended exposure to atmospheric O_2.

RESULTS AND DISCUSSION

CO_2 conversion (panel a) and yields of CO (panel b) and CH_4 (panel c) obtained in the temperature programmed CO_2 reduction experiments on 0.1, 0.5, 1, 2, and 5 wt % Ru/Al_2O_3 samples are displayed in Figure 1. On the 5% Ru/Al_2O_3 catalyst, the CO_2 reduction starts at ∼150 °C and shows the maximum conversion at ∼320 °C, and then, the conversion decreases with further temperature increase to ∼500 °C. Above 500 °C, the CO_2 conversion increases again. With decreasing Ru loading, the CO_2 conversion profiles are shifted toward higher temperature. On the 0.1 wt % Ru/Al_2O_3 sample, CO_2 reduction starts above ∼300 °C and monotonically increases and then slows down above 450 °C. CO_2 conversion levels above this temperature (∼450 °C) are practically the same for all Ru loadings studied, although the loading changes by a factor of 50. Even though CO formation starts at practically the same temperature (∼300 °C) for all Ru-loaded samples, the activity profiles were very different. Interestingly, catalysts with a lower amount of Ru showed a significantly higher rate of CO formation at relatively low temperature, while over Ru/Al_2O_3 catalysts with Ru loading ≥2% the CO yield increased monotonically. The highest CO yield in the 350−500 °C temperature range was observed for the lowest Ru-loaded sample (0.1%). The CO yield increased rapidly after the onset temperature of ∼350 °C, but then, it leveled off between 450 and 500 °C, and at even higher temperatures, it followed exactly the same path we observed for all the other catalysts. When the Ru loading increased to 0.5%, the trend in the CO yield was similar to that observed for the 0.1% sample; however, its initial high activity leveled off at a much lower CO yield than that seen for the 0.1% catalyst. For the 1% sample, the high CO yield region at low temperature is even less evident than over the other two low Ru-loaded samples, but it is still clearly distinguishable. Above 500 °C, the CO yield profiles are identical for all catalysts studied and practically fall on a single line. The CH_4 yield profiles indicate that methane formation rate increases with increasing Ru loading and, at the same time, the temperature where the maximum methane yield is observed shifts to lower values with increasing Ru loading. These temperature programmed reaction results were completely consistent with our previously reported results on CO_2 reduction on Pd/alumina, where we have unambiguously showed that isolated, single Pd atoms favor the formation of CO, while methane formation is prevalent on Pd clusters. These results are very peculiar in light that Ru has been well-known as a very efficient methanation catalyst.[15] The CO_2 conversion as well as the CO and CH_4 yields trends seem to suggest the existence of three different reaction regimes as the temperature is increased from 25 to 500 °C. The formation of CH_4 is prevalent at low reaction temperatures, and the CH_4 yield increases proportionally with Ru loading. This is in line with the conclusions of earlier studies that CH_4 formation is favored on large metal clusters. With increasing Ru loading, the size of metal clusters increases, as it has been substantiated by TEM measurements. At very low Ru loading (0.1 wt %) (highly dispersed Ru), no CH_4 formation is seen even at temperatures (∼350 °C) where the CH_4 yield reached its maximum at high Ru loadings. As we will show in the following paragraph, the low Ru-loaded catalyst exhibits CH_4 formation activity only after the onset of metal sintering, i.e., after the formation of 3D metal clusters. The maximum in the CO_2 conversion vs temperature plot can solely be attributed to the maximum in CH_4 formation rate. This behavior suggests that at high temperature the concentration of one of the reactants (either CO_2 or H_2) on the catalyst surface decreases which leads to a drop in CO_2 conversion and also in the CH_4 yield. In the second temperature regime, the dominant reaction is the formation of CO on highly dispersed Ru particles. At low Ru loadings, we see a particular shape of the CO yield traces as a function of temperature. The onset temperature of CO formation at low Ru loadings is around 320 °C. At the lowest Ru loading (0.1 wt %), the CO yield increases fast with temperature, levels off around 450 °C, and then increases again above 500 °C. With increasing Ru laoding, however, the CO yield drops, and over the 5 wt % Ru-loaded sample, we observe no CO formation. CO is only produced on this sample as a result of a secondary reaction at this high temperature between CH_4 formed on Ru clusters and the reactant CO_2 (dry reforming of CO_2). (The observed increase in CO yield above 500 °C over the low Ru loaded samples can also be attributed to the onset of this secondary reaction.) The increase in CO_2 conversion at high temperatures (above 500 °C) on all samples studied here can be attributed to the reaction between CH_4 and CO_2.

CO_x methanation over supported Ru catalysts has been shown to be structure sensitive as it depended on the particle size of Ru clusters.[16−21] For CO hydrogenation, Che et al.[21] observed that the TOF decreased with increasing Ru dispersion, and similar findings for CO_2 methanation were reported by Kowalczyk et al.[16] (although, in the latter study, the size of Ru clusters was shown to affect the CO_2 hydrogenation rate in a lesser extent than the rate of CO hydrogenation). The variation in the methanation rate with Ru particle size might be (at least in part) correlated with the effect of the support on the metal particles. The electronic state (charge density) of the Ru particles on a given support material (here Al_2O_3) may vary with particle size, as it was proposed by Scire at al.,[22] who reported that the electronic state of the active metal (Ru) strongly influenced the CO selectivity in the CO_2 hydrogenation process. They proposed that a more oxidized Ru surface led to higher methanation activity, due to the higher hydrogen and lower CO coverage. In order to vary the electronic properties of Ru particles supported on YSZ solid electrolyte pellets, Theleritis et al.[23] used the electrochemical promotion of catalysis (EPOC) effect by applying external potential to the catalytic system. They found that at low temperatures (up to 240 °C) CO_2 hydrogenation reaction yielded CH_4 primarily, while CO was the dominant product at high temperatures. Electrochemical O^{2-} supply to the Ru

dx.doi.org/10.1021/cs400381f | ACS Catal. 2013, 3, 2449−2455

particles resulted in large increases in both the formation rate and selectivity of CH_4 and concomitantly a large decrease in the CO formation rate.

The results of these temperature programmed reaction measurements may also be argued on the basis of having more Ru in the catalyst translating to higher hydrogenation activity and, therefore, extensive CH_4 formation. This interpretation, however, cannot explain the formation of the larger amount of CO on catalysts containing a lower amount of Ru. In order to address this issue, we performed isothermal CO_2 hydrogenation on the 0.1% Ru/Al_2O_3 catalyst at 350 °C. At this temperature, single Ru atoms present on the alumina support initially show sintering during the course of reaction. The initial selectivity of CO formation at this catalyst bed temperature is much higher (over 84%) than that of CH_4 production on the 0.1% Ru/Al_2O_3 catalyst, as shown in Figure 2a. With increasing time-on-stream, CO production rate increased slowly, while the CH_4 formation rate increased much faster, and after ~200 min time-on-stream, CO and CH_4 were produced in almost the same amounts. After 16 h time-on-stream, CH_4 production far exceeded the formation of CO, as the CO selectivity dropped to ~36%.

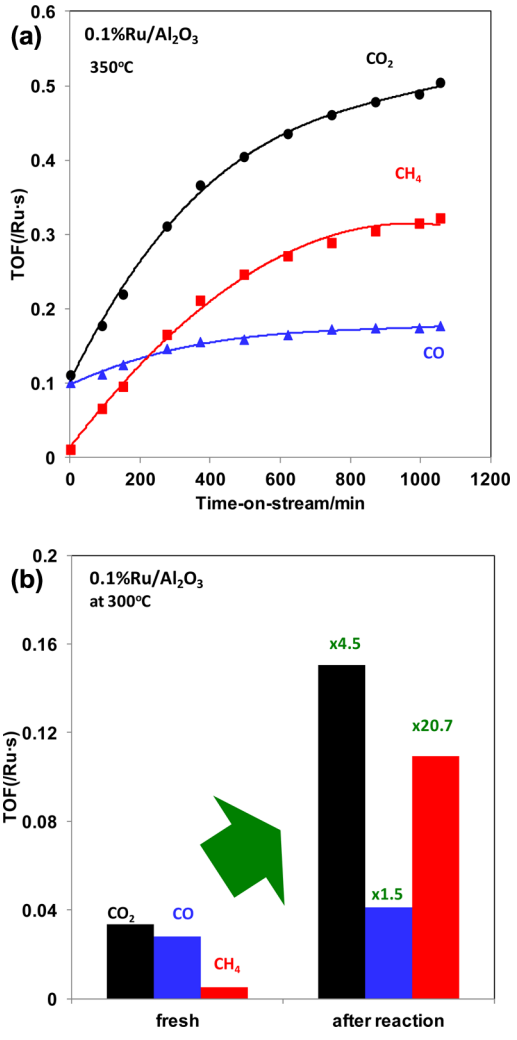

Figure 2. (a) TOFs of CO_2, CO, and CH_4 as a function of time-on-stream at 350 °C over a 0.1% Ru/Al_2O_3 catalyst. (b) Steady state TOFs for CO_2 conversion and CO/CH_4 production over a fresh and reactivated (after reaction at 350 °C) 0.1% Ru/Al_2O_3 catalyst at 300 °C.

These results indicate that the Ru/Al_2O_3 catalysts with low Ru loadings are not stable under the reducing reaction conditions of CO_2 reduction. In order to compare the activities of fresh and used catalysts, we evaluated the steady state activities of two 0.1% Ru/Al_2O_3 catalysts at 300 °C: a freshly prepared catalyst and the one that was reactivity tested at 350 °C for 16 h. The fresh catalyst showed stable steady state activity at this lower reaction temperature of 300 °C in comparison to that observed at 350 °C. As the results of Figure 2b substantiate, the overall CO_2 conversion activity of the 350 °C-tested catalyst increased ~4.5 times and most of the activity increase came from the ~20-fold increase in the CH_4 production rate. At the same time, the increase in CO TOF at steady state at 300 °C over the 350 °C-tested sample was much smaller, only about 1.5×. A likely explanation for the observed variation in catalytic activity at high temperature with time-on-stream is the change in metal particle size under reaction conditions. As we have seen for the Pd/Al_2O_3 catalysts,[11] both the overall catalytic activity (i.e., CO_2 conversion) and the product (CO and CH_4) selectivity were strongly dependent on the active metal particle size. In order to visualize the change in metal particle size (changes in Ru dispersion), we collected STEM images from two catalyst samples: from a freshly prepared 0.1% Ru/Al_2O_3 catalyst and from the one that was reaction-tested at 350 °C. The freshly prepared 0.1% Ru/Al_2O_3 sample showed almost exclusively atomically dispersed Ru (and very small Ru aggregates) on the alumina support (Figure 3a). On the

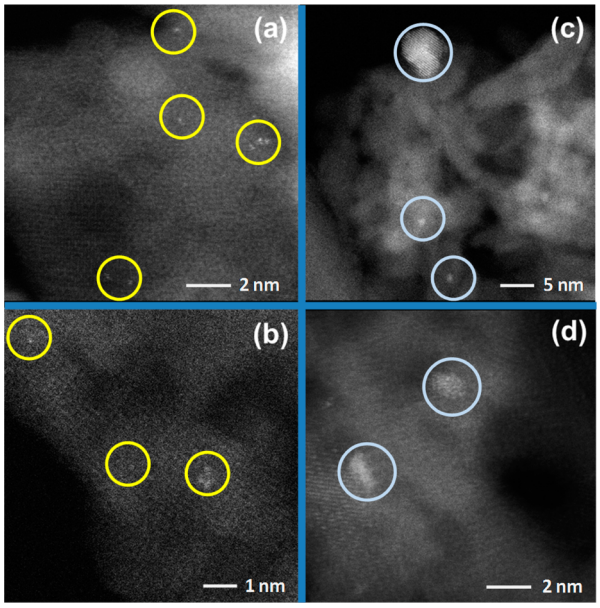

Figure 3. STEM images from a 0.1% Ru/Al_2O_3 catalyst before (images a and b) and after (images c and d) CO_2 reduction at 350 °C for 16 h.

contrary, after reaction test at 350 °C for 16 h, mostly nm-sized (some of them even larger than 5 nm) 3D Ru clusters are visible in the STEM images (Figure 3c). These results strongly support our hypothesis that CO formation is favored on single Ru atoms supported on alumina, while Ru clusters are mostly active for CH_4 formations. Therefore, we conclude that the high methanation activity reported for Ru on alumina catalysts originate from large (3D) Ru clusters. The catalytic data discussed in the previous section seem to suggest that the reaction mechanism is different for the small (atomically dispersed) and larger (3D) Ru particles. Therefore, next we

dx.doi.org/10.1021/cs400381f | ACS Catal. 2013, 3, 2449−2455

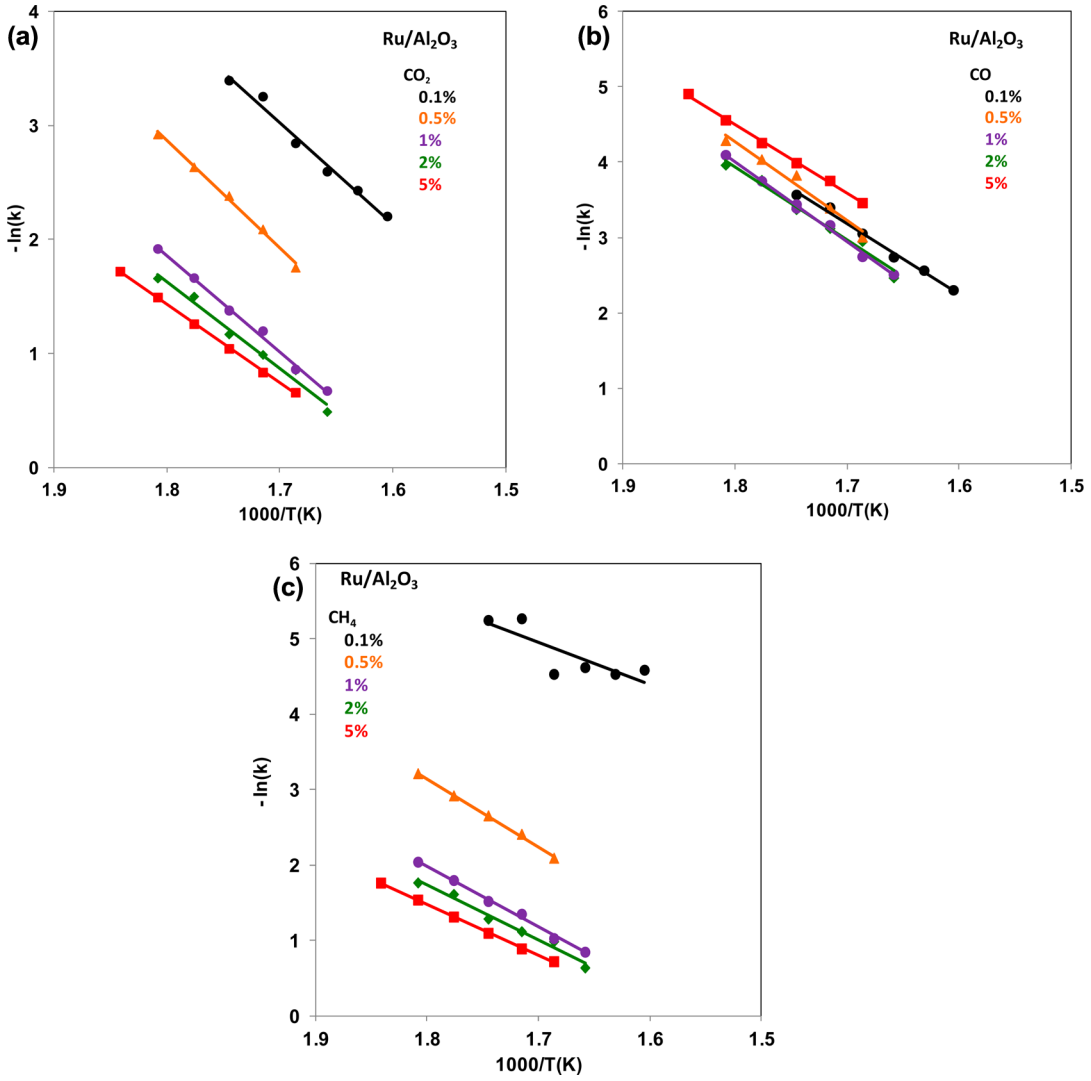

Figure 4. Arrhenius plots for CO_2 conversion (a), as well as for CO (b) and CH_4 (c) formations over Ru/Al_2O_3 catalysts between 270 and 350 °C.

investigated how the reaction mechanisms changed with the variation of active metal particle size. To this end, we performed kinetic measurements on all the Ru-loaded alumina supported catalysts prepared (from 0.1 to 5% Ru loading). A series of Arrhenius plots of CO_2 TOF (calculated on the basis of the number of surface Ru atoms on the alumina supported metal clusters) are displayed in Figure 4a, each showing reasonable linearity in the temperature regime explored in this study (270−350 °C). The CO_2 TOF is the lowest over the 0.1 wt % Ru/alumina catalyst and increases dramatically over the 0.5 wt % sample and further over the 1 wt % catalyst. Above 1 wt % Ru loading, the CO_2 TOF increases only marginally. Good linearity in the Arrhenius plots for both CO and methane TOFs is shown in Figure 4b,c, respectively, except for the 0.1% Ru/Al_2O_3 sample which is related to the significant error in the calculation of TOF due to low CH_4 selectivity. At Ru loadings up to 2%, the CO TOF values are very similar and only drop significantly on the highest Ru loaded sample (5 wt %), as large metal clusters tend to produce no CO. The TOF plots of CH_4 at Ru loadings higher than 1% are very close to each other, but there is a systematic increase in CH_4 TOF with increasing Ru loading. This observation suggests that Ru clusters exhibit very similar catalytic activities toward CH_4 formation above a certain cluster size. These results are consistent with our previous interpretations that single Ru atoms or interfacial Ru favor CO formation, while Ru clusters favor CH_4 formation. From the slopes, we can estimate the apparent activation energies of CO and CH_4 formation. Interestingly, the activation energy for CO formation (~82 kJ/mol) was always ~20 kJ/mol higher than that for CH_4 formation (~62 kJ/mol), regardless of Ru loading. If one considers CO as an intermediate in the path toward CH_4 formation in the CO_2 hydrogenation process, the activation energy for CO formation should be equal to or lower than that for CH_4 formation. Therefore, we propose that CO is formed either by a different route (not as an intermediate in the reduction toward CH_4) or on a different active center than CH_4. The E_a for methane formation obtained from the Arrhenius plots in this study is comparable to those reported previously by Solymosi et al.[24,25] for CO_2 methanation over 5% Ru/Al_2O_3 (67.4 kJ/mol) and by Bartholomew et al.[26] for Ru/SiO_2 (72 kJ/mol). Changes in the apparent activation energy with reaction conditions applied has also been reported in the latter publication due, possibly, to the variation in the rate determining step under different reaction conditions.

In Figure 5a, we show CO and CH_4 TOFs measured at 300 °C as a function of Ru loading in the reduction of CO_2. With increasing Ru loading, the trends in CO and CH_4 TOFs are opposite: the TOF for CO formation is practically constant up

dx.doi.org/10.1021/cs400381f | ACS Catal. 2013, 3, 2449−2455

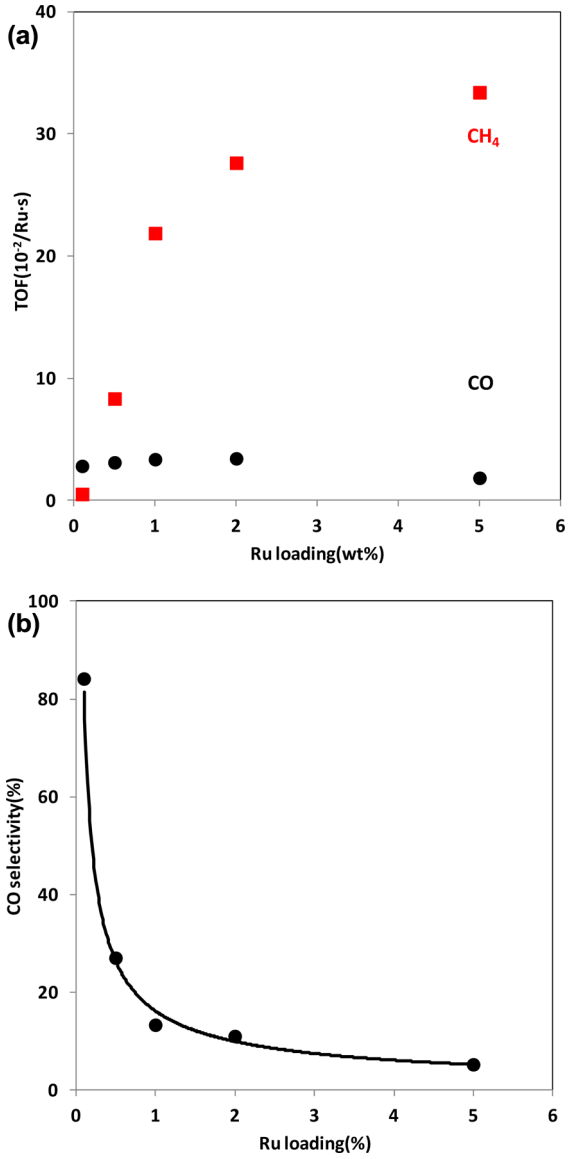

Figure 5. (a) TOFs of CO and CH_4 formation at steady state at 300 °C over Ru/Al_2O_3 catalysts as a function of Ru loading (open symbols: data obtained form a 0.1% Ru/Al_2O_3 catalyst that was tested previously at 350 °C). (b) CO slectivity as a function of Ru loading at 300 °C.

to 2 wt % Ru loading and then it decreases, while that for CH_4 formation increased in the entire Ru loading regime studied (0.1−5 wt %). The CO selectivity below 1% Ru on alumina evidently increases sharply with the decrease in Ru loading (Figure 5b). We believe that these results indicate high Ru dispersion at loadings less than 1%, when most of the Ru is present as isolated single atoms and small metal aggregates, and the production of CO is favored. On the other hand, at Ru loadings high enough to form Ru clusters (starting from ∼1%), the reduction of CO_2 proceeds all the way to CH_4. These results are fully consistent with our previous report on the reactivity of isolated Pd atoms that have been shown to favor the formation of CO, while mostly CH_4 formed on the Pd clusters.[11] The results of both of these studies strongly suggest that the active sites for CO formation are highly dispersed single metal atoms (these form CO with high selectivity) and possibly small metal aggregates, as well. However, the formation of CH_4 can only proceed in the presence of metal clusters that are able to supply large amounts of atomic hydrogen to this process. As we have mentioned above, the apparent activation energy for CH_4 formation is about 20 kJ/mol lower than that of CO formation over every Ru/Al_2O_3 catalyst studied here. This result seems to suggest that CH_4 production may not proceed through an intermediate that formed from CO produced in the initial reduction step. To test this, we performed temperature programmed reduction of both CO and CO_2 on freshly prepared 0.1% Ru/Al_2O_3 catalysts. As the results displayed in Figure 6 show, the onset temperature

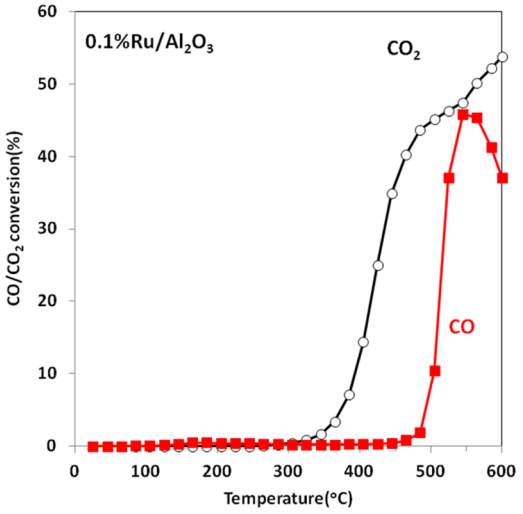

Figure 6. Temperature programmed CO and CO_2 conversions over a 0.1% Ru/Al_2O_3 catalyst.

for CO_2 hydrogenation on the 0.1% Ru/Al_2O_3 is ∼300−350 °C, while that for CO hydrogenation is ∼500 °C. We propose that this ∼150 °C upward shift in the on-set temperature for hydrogenation provides two important insights into the reaction mechanisms. First, CO_2 hydrogenation to CO might proceed by two different, in parallel occurring mechanisms: hydrogenation on metallic surfaces and reverse water gas shift reaction. Second, alumina-supported isolated single Ru atoms can catalyze CO_2 reduction to CO but cannot catalyze further hydrogenation to CH_4 due, perhaps, to their limited hydrogen activation functionality. This would be consistent with our previous finding[11] in that dual catalyst functionality was required for CO_2 hydrogenation to CH_4 over supported Pd catalysts. In a Ru-doped ceria catalyst, Metiu et al.[27] have also found that "gas-phase CO is not a reaction intermediate for the methanation of CO_2 by $Ce_{0.95}Ru_{0.05}O_2$". In a recent study, Ussa Aldana et al. carried out in operando FTIR measurements on the CO_2 methanation reaction over $Ni/CeZrO_2$ catalysts.[28] Their results unambiguously show that methane formation does not go through a CO intermediate, rather surface carbonate/formate species formed on the oxide support play a critical role in the formation of CH_4. Adsorbed CO_2 is proposed to hydrogenate stepwise, forming bicarbonates, formates, formaldehyde, and finally methoxide. Supported Ni clusters dissociate H_2 and supply H atoms for these hydrogenation steps. The mechanism of CO_2 methanation on supported Ru catalysts has also been strongly debated, and no clear consensus on the actual reaction path has been reached. On the basis of the results of a DRIFT spectroscopy study, Prairie et al. proposed formic acid as a critical intermediate in

dx.doi.org/10.1021/cs400381f | ACS Catal. 2013, 3, 2449−2455

the CO_2 methanation process.[29] Subsequently, the role of formic acid or formate intermediate was questioned by Traa et al., who found in their kinetic study on CO_2 methanation over Ru/TiO_2 catalysts that CH_4 formation proceeded through the hydrogenation of surface carbon as the rate determining step.[30] Our current kinetic and spectroscopy studies are focused on understanding the reaction mechanisms for the formation of both CO and CH_4 over these Ru-based catalysts at different Ru loadings and identifying active catalytic centers of these materials and key reaction intermediates.

CONCLUSION

The reactivities of Ru/Al_2O_3 catalysts in the Ru loading range of 0.1−5 wt % were studies in the reduction of CO_2 with H_2. The main focus of the work was to find correlation between the active metal dispersion and the catalytic performance of these materials. At very high metal dispersion (metals mostly present in atomic dispersion, as evidence by STEM), the catalyst produces CO with high selectivity. As 3D metal clusters form at higher Ru loadings (at and above 1 wt %) or as a results of sintering, the selectivity toward CH_4 formation increases significantly. Catalysts with low metal loading, however, are unstable under reaction conditions of CO_2 reduction and form large metal clusters. This clustering is accompanied by a large increase in CH_4 selectivity and drop in CO formation selectivity. Apparent activation energies of 82 and 62 kJ/mol were estimated from the slopes of Arrhenius plots for CO and CH_4 formation, respectively. The difference in activation energy of ∼20 kJ/mol for each catalyst studied suggests either different reaction paths for the formation of CO and CH_4 and/or different active sites. The higher apparent activation energy for CO formation also seems to suggest that CO is not an intermediate in the formation of CH_4. This is further supported by the results of activity measurements over a 0.1% Ru/Al_2O_3 catalyst, that showed about a 125 °C onset temperature difference between the CO_2 (∼325 °C) and CO (∼450 °C) reduction.

AUTHOR INFORMATION

Corresponding Authors

*E-mail: jhkwak@unist.ac.kr.
*E-mail: janos.szanyi@pnnl.gov.

Present Address

[#]J.H.K.: School of Nano-Bioscience and Chemical Engineering, UNIST, 100 Banyeon-Ri, Ulsan 689-798, Korea.

Notes

The authors declare no competing financial interest.

ACKNOWLEDGMENTS

We thank Dr. Feng Gao for carrying out the H_2 chemisorption measurements on all the Ru/Al_2O_3 catalysts discussed in this work. The catalyst preparation and catalytic measurements were supported by a Laboratory Directed Research and Development (LDRD) project, while the TEM work was supported by the Chemical Imaging Initiative at the Pacific Northwest National Laboratory (PNNL). PNNL is operated for the US Department of Energy by Battelle Memorial Institute under contract number DE-AC05-76RL01830. J.H.K. also acknowledges the support of this work by the 2013 Research Fund of UNIST (Ulsan National Institute of Science and Technology, Ulsan, Korea).

REFERENCES

(1) Boffa, A.; Lin, C.; Bell, A. T.; Somorjai, G. A. *J. Catal.* **1994**, *149*, 149.
(2) Wambach, J.; Baiker, A.; Wokaun, A. *Phys. Chem. Chem. Phys.* **1999**, *1*, 5071.
(3) Sneeden, R. P. A. *J. Mol. Catal.* **1982**, *17*, 349.
(4) Fisher, I. A.; Bell, A. T. *J. Catal.* **1996**, *162*, 54.
(5) Baiker, A. *Appl. Organomet. Chem.* **2000**, *14*, 751.
(6) Peterson, A. A.; Abild-Pedersen, F.; Studt, F.; Rossmeisl, J.; Norskov, J. K. *Energy Environ. Sci.* **2010**, *3*, 1311.
(7) Durand, W. J.; Peterson, A. A.; Studt, F.; Abild-Pedersen, F.; Norskov, J. K. *Surf. Sci.* **2011**, *605*, 1354.
(8) Ferrin, P.; Mavrikakis, M. *J. Am. Chem. Soc.* **2009**, *131*, 14381.
(9) Clarke, D. B.; Bell, A. T. *J. Catal.* **1995**, *154*, 314.
(10) Clarke, D. B.; Suzuki, I.; Bell, A. T. *J. Catal.* **1993**, *142*, 27.
(11) Kwak, J. H.; Kovarik, L.; Szanyi, J. *ACS Catalysis* **2013**, *3*, 2094−2100.
(12) Solymosi, F.; Erdőhelyi, A.; Kocsis, M. *J. Chem. Soc.-Faraday Trans.* **1981**, *77*, 1003.
(13) Elliott, D. J.; Lunsford, J. H. *J. Catal.* **1979**, *57*, 11.
(14) Kusmierz, M. *Catal. Today* **2008**, *137*, 429.
(15) Mills, G. A.; Steffgen, F. W. *Catal. Rev.* **1973**, *8*, 159.
(16) Kowalczyk, Z.; Stolecki, K.; Rarog-Pilecka, W.; Moskiewicz, E.; Wilczkowska, E.; Karpinsky, Z. *Appl. Catal., A: Gen.* **2008**, *342*, 35.
(17) King, D. L. *J. Catal.* **1978**, *51*, 386.
(18) Kellner, S. C.; Bell, A. T. *J. Catal.* **1982**, *75*, 251.
(19) Guczi, L.; Schay, Z.; Matusek, K.; Bogyai, I. *Appl. Catal.* **1986**, *22*, 289.
(20) Venter, J. J.; Vannice, M. A. *Inorg. Chem.* **1989**, *28*, 1634.
(21) Che, M.; Bennett, C. O. *Adv. Catal.* **1989**, *36*, 55.
(22) Scire, S.; Crisafulli, C.; Maggiore, R.; Minico, S.; Galvagno, S. *Catal. Lett.* **1998**, *51*, 41.
(23) Theleritis, D.; Souentie, S.; Siokou, A.; Katsaounis, A.; Vayenas, C. G. *ACS Catal.* **2012**, *2*, 770.
(24) Solymosi, F.; Erdőhelyi, A. *J. Mol. Catal.* **1980**, *8*, 471.
(25) Solymosi, F.; Erdőhelyi, A.; Bánsági, T. *J. Catal.* **1981**, *68*, 371.
(26) Weatherbee, G. D.; Bartholomew, C. H. *J. Catal.* **1984**, *87*, 352−362.
(27) Sharma, S.; Hu, Z.; Zhang, P.; McFarland, E. W.; Metiu, H. *J. Catal.* **2011**, *278*, 297.
(28) Ussa Aldana, P. A.; Ocampo, F.; Kolb, K.; Louis, B.; Thibault-Starzyk, F.; Daturi, M.; Bazin, P.; Thomas, S.; Roger, A. C. *Catal. Today* **2013**, *215*, 201−207.
(29) Prairie, M. R.; Renken, A.; Highfield, J. G.; Thampi, K. R.; Grätzel, M. *J. Catal.* **1991**, *129*, 130.
(30) Traa, Y.; Weitkamp, J. *Chem. Eng. Technol.* **1999**, *21*, 4.